

PROCESS OPTIMISATION AND DESIGN OF A BELT FURNACE FOR NICKEL OXIDE REDUCTION

Ross HAYWOOD Ph.D.

Hatch Associates Pty Limited, Brisbane, Qld 4000, AUSTRALIA

ABSTRACT

A computational fluid dynamic model has been developed to simulate the operation of a travelling-belt furnace used in the production of nickel metal powder by the reduction of nickel oxide. The model, based on a commercial CFD code, includes the effects of heat transfer by convection, conduction and radiation, bulk motion of the solids on the belt and a simple kinetic scheme to describe carbon gasification and nickel reduction processes. Plant and laboratory data used in developing and validating the model are described. The model has been used in the development of an optimised process and to improve the furnace design within a new production facility.

NOMENCLATURE

C_p	specific heat
k	thermal conductivity
r	reaction rate
R	thermal contact resistance
\mathcal{R}	universal gas constant
S_ϕ	general source term
T	temperature
T_{amb}	ambient temperature
U_{belt}	bed/belt velocity
u	horizontal velocity component
v	vertical velocity component
\vec{V}	velocity
X	volume fraction
Y	mass fraction
Y_C	solid phase carbon mass fraction
Y_{NiO}	solid phase nickel oxide mass fraction
Y_O	solid phase oxygen mass fraction
α_C	carbon gasification reaction rate factor
α_O	nickel oxide reduction reaction rate factor
Γ_ϕ	general scalar diffusivity
Φ	general scalar
ρ	density

INTRODUCTION

Travelling-belt, tray, and grate furnaces have widespread application in the minerals processing and metallurgical industries. At their Yabulu refinery, Queensland Nickel Pty Limited (QNPL) currently use travelling-belt furnaces, both for the final reduction of nickel oxide powder and to sinter compacted nickel rondelles (the final product).

Similar process technology, at an appreciably larger scale, is being considered in the feasibility study of a proposed brownfield expansion of the facilities.

In the existing reduction furnace a nickel-oxide powder (calcine) and sawdust is deposited at a depth of up to 50mm across the full width of a stainless steel strip belt, which moves at a uniform speed (of order 0.02 m/s) through the furnace. Electrical radiant elements heat the calcine bed both above and below the belt while a hydrogen-nitrogen atmosphere accomplishes the reduction to nickel metal. Seals at each end of the furnace are purged with an inert gas to prevent accumulation or leakage of flammable gas mixtures. A typical cross sectional schematic of a travelling-belt reduction furnace is shown in Figure 1. Furnaces of this type are typically 50 to 100 metres in length with belt widths of up to 2 metres.

To ensure a successful scale-up for the new furnace and in view of some uncertainties in the relative rates of heat transfer and chemical reaction, a significant part of the QNPL expansion feasibility study has been directed at improving the understanding of nickel oxide powder reduction in a belt furnace at a very fundamental level. This has included the development of a comprehensive process model to provide guidance in optimising the process conditions and basic design of the new furnace.

MODEL DESCRIPTION

The model is based on a two-dimensional representation of the travelling-belt furnace. The domain includes the furnace refractories, radiant elements, gas-space, calcine/sawdust bed, belt, and rollers.

The model solves the mass and momentum equations including the standard k-epsilon model for turbulence in the gas-phase while a constant and uniform velocity field is specified for the bed and belt. The gas and bed/belt are counter flowing.

In the bed and belt, heat transfer by conduction and convection are considered, the latter due to the specified velocity field. In the gas-phase the effects of radiative heat transfer are included through the use of a discrete ordinates (finite volume) model in addition to conduction and convection.

Within the calcine/sawdust bed the important chemical reactions of oxide reduction and carbon (sawdust)

gasification occur. Reduction of nickel oxide is predominantly by the action of gaseous hydrogen that diffuses into the bed from the gas-phase followed by counter diffusion of water vapour that is created as a by-product of the reduction process. The sawdust, which is mixed with the calcine to enhance gaseous diffusion within the bed, is essentially a contaminant that is undesirable in the final product and must be removed. The primary means of carbon consumption is through gasification with the water vapour generated from oxide reduction. Of less importance in the reduction and

gasification processes is the cyclic reduction whereby carbon monoxide acts to reduce the nickel oxide, generating carbon dioxide, which then acts to consume bed carbon and generate further carbon monoxide. The two nickel oxide reduction and two carbon gasification reactions are given in equations 1 to 4. Note that the gasification reactions are strongly endothermic whereas the reduction reactions are mildly exothermic at the temperatures of interest.

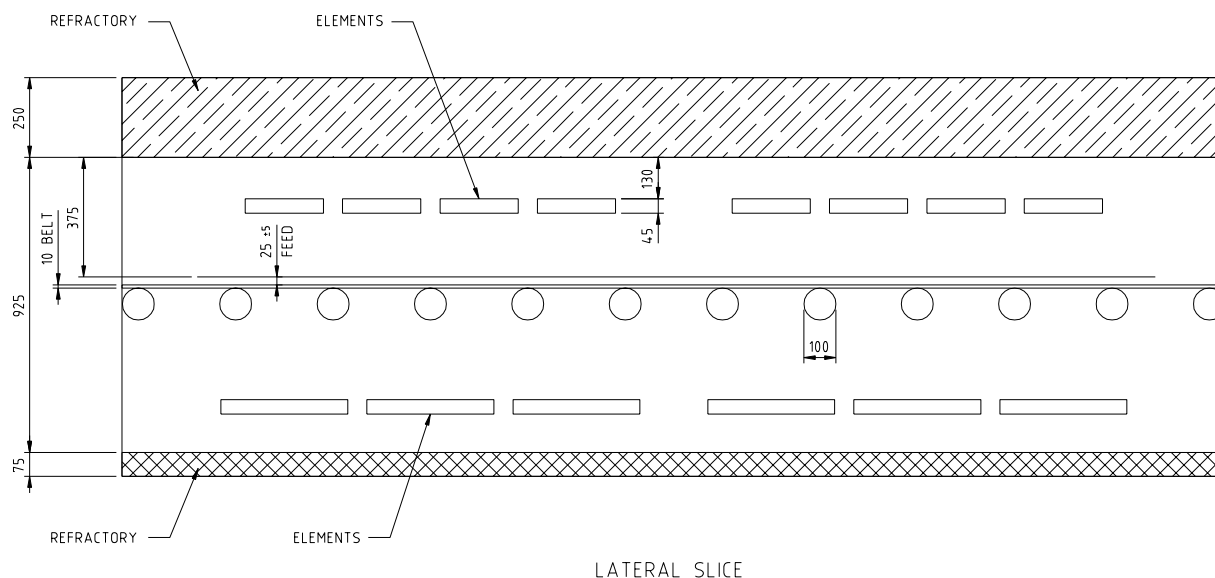


Figure 1 Schematic Cross Section of Travelling-belt Reduction Furnace. All dimensions in mm.



$$-13 \text{ MJ/kmol @ } 800 \text{ }^\circ\text{C}$$



$$-47 \text{ MJ/kmol @ } 800 \text{ }^\circ\text{C}$$

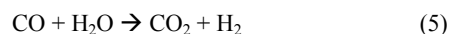


$$+169 \text{ MJ/kmol @ } 800 \text{ }^\circ\text{C}$$



$$+135 \text{ MJ/kmol @ } 800 \text{ }^\circ\text{C}$$

temperatures ($900 \text{ }^\circ\text{C}$) it would be reasonable to expect that the water-gas shift reaction (Equation 5) is active, particularly within the solid bed where it would be catalysed by the presence of high temperature nickel metal. However, in light of the expected near equilibrium behaviour of this reaction under process conditions and the fact that species participating in both the reduction (H_2 and CO) and carbon gasification reactions (H_2O and CO_2) appear as both reactants and products in Equation 5, the water-gas shift reaction has not been modelled.



$$-33 \text{ MJ/kmol @ } 800 \text{ }^\circ\text{C}$$

Assumptions

The following assumptions have been made in developing the model:

- Edge effects are not significant and the total furnace can be adequately modelled in two dimensions.
- Constant density has been assumed in gas- and solid-phases.
- Constant porosity in the solid-phase with no changes due to sintering, void formation or fissure generation within the bed.

In practice the primary function of the gas-phase is to provide the appropriate reducing atmosphere and continuously remove the by-products of reduction. For the purposes of the current model chemical reactions in the gas-phase have been ignored. At typical bed

- Constant diffusibility (ratio of actual in-bed gaseous to theoretical free-space diffusion coefficient) in the solid phase. Hoogshagen, (1955)
- Uniform and constant velocity of the belt and bed material.
- No gaseous exchange (infiltration or leakage) between furnace internal and environment.
- No resistance to mass transfer at the gas/bed interface (ie specified gaseous mass fractions at the bed surface)
- A finite volume model of thermal radiation (discrete ordinates) has been used.
- There is a small but finite thermal resistance at the bed/belt interface to model the effects of the contact resistance.
- Constant thermal properties (thermal conductivity, specific heat, and emissivity) have been assumed for the reducing gas, belt, rollers, and refractory.
- Piecewise linear approximations have been used to express the variation with temperature of the calcine thermal conductivity and specific heat.
- Piecewise linear approximations have been used to express the variation with temperature of the diffusion coefficients in the equations governing transport of gaseous species within the bed.
- The fundamental chemical reactions included in the model are the reduction of solid nickel-oxide by hydrogen and carbon-monoxide and the gasification of solid-phase carbon by water-vapour and carbon-dioxide (Equations 1-4).
- Arrhenius expressions have been used for the rates of reduction and carbon gasification reactions. Reduction rates are based on the work of Rashed and Rao (1996).
- All gas-phase reactions have been ignored including the water-gas shift reaction and heterogeneous reactions leading to soot formation.

Table 2 lists the boundary conditions used in the model.

Supporting Analytical Work

Where possible, literature values were used in the specification of thermophysical properties used in the model, particularly for properties where there was confidence that reported values were reasonably representative or for those properties where the model predictions were expected to be relatively insensitive. However, the process and model sensitivity to the fundamental calcine thermal properties and chemical kinetic parameters suggested that detailed bench-scale

testwork to develop values specific to the actual materials would be prudent.

Thermal properties of the QNPL calcine/sawdust mixtures were examined in detail at the Thermal Property Research Laboratory, West Lafayette IN. Specifically, a heated probe method and a differential scanning calorimeter were used to determine the calcine/sawdust thermal conductivity and specific heat respectively over the temperature range from 25 to 800 °C. Piecewise linear approximations to the experimental results were developed and used directly in the CFD model.

Similarly, the sawdust behaviour, both pyrolysis and resulting char reactivity, was investigated by CSIRO Energy Technology. Tests using a thermogravimetric analyser determined the pyrolysis profile of the sawdust yielding the volatile yield-temperature history at heating rates comparable to the real furnace system. A fixed bed reactor was then used to determine the reactivity of the sawdust char. Pre-exponential factors, activation energy and reaction order were determined for reactivity with both CO₂ and H₂O. Details of the method can be found in Harris and Smith (1990) and Roberts and Harris (2000). The results showed the sawdust char to be considerably more reactive than bituminous coal chars prepared under similar conditions. The observed high reactivity was partially because the sawdust generates a char with a high specific surface area, however even allowing for surface area effects the sawdust char exhibited a very high intrinsic (normalised to char surface area) reactivity.

Software

An unstructured grid was developed using the FLUENT pre-processor GAMBIT. A section of the grid is shown in Figure 2.

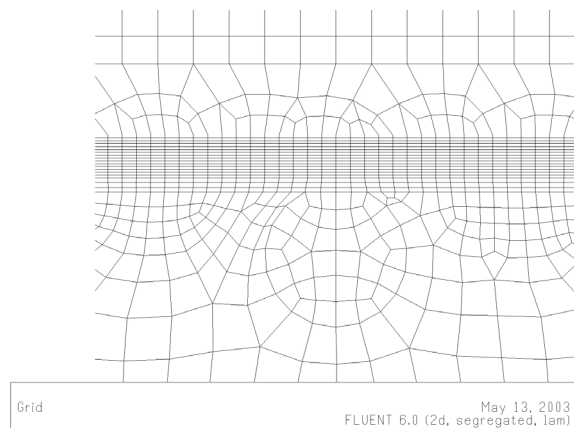


Figure 2: Computational grid showing feed material, belt, and rollers.

The important calcine bed was resolved with a 2 mm vertical control volume spacing. The entire computational grid consisted of approximately 200,000 quadrilateral elements. FLUENT v6 was used as the basis of the computational model. The “User-Defined Scalar” (UDS) facility was used to model the transport and conversion of calcine and sawdust. Conservation equations for solid-phase oxygen and carbon mass fraction were developed and are given in Table 1. The source terms account for

the consumption of solid-phase oxygen and carbon due to the reduction and gasification reactions respectively. The reaction rate factors α_O and α_C are an empirical correction to account for the observed asymptotic decline in reduction and gasification rates at high levels of conversion. In addition to the two UDS's for the solid-phase components of interest, five UDS's were defined for the gas-species present within the bed (H_2 , H_2O , CO , CO_2 , N_2). The conservation equations for the gas species used an effective diffusion coefficient based on the diffusibility

concept for porous materials of Hoogshagen, (1955). The gas-species conservation equations are very similar to those given for the solid phase and are omitted here in the interest of brevity. Coupling of the source terms in the conservation equations for the complete set of seven UDS's led to some numerical instability and modest under-relaxation was required to achieve converged solutions. Convergence was assumed when the maximum residuals were less than 10^{-5} in all equations.

Table 1: Governing equation, diffusivities, and source terms for Bed Solids Composition

$\frac{\partial(\rho\Phi)}{\partial t} + \vec{\nabla} \cdot (\rho\vec{v}\Phi) = \vec{\nabla} \cdot (\Gamma_\Phi \vec{\nabla}\Phi) + S_\Phi$		
Φ	Γ_Φ	S_Φ
Y_O	0	$-\rho Y_{NiO}(r_1 + r_2)$
Y_C	0	$-\rho Y_C(r_3 + r_4)$
$r_1 = \alpha_O X_{H_2} \cdot 90,000 \exp(-100,000/\mathcal{R}T)$	(kg O)/(kg NiO)/s	
$r_2 = \alpha_O X_{CO} \cdot 90,000 \exp(-100,000/\mathcal{R}T)$	(kg O)/(kg NiO)/s	
$r_3 = \alpha_C (X_{H_2O})^{0.5} \cdot 2 \times 10^8 \exp(-220,000/\mathcal{R}T)$	(kg C)/(kg C)/s	
$r_4 = \alpha_C (X_{CO_2})^{0.3} \cdot 9 \times 10^{11} \exp(-318,000/\mathcal{R}T)$	(kg C)/(kg C)/s	

Table 2: Boundary conditions

Parameter	Kinematic B.C.	Thermal B.C.	Gas/Solids Species B.C.
Gas Inlet	$u = -4.6$ $v = 0.0$	Temperature Specified $T = 500^\circ C$	Specified Composition, $Y_{H_2}=0.2, Y_{N_2} = 0.8$
Gas Outlet	Outlet condition	Zero Gradient, $\delta T/\delta x=0$	Zero gradient, $\delta Y/\delta x=0$
Feed Inlet	$u = U_{belt}$	Temperature Specified $T = 30^\circ C$	Specified Solids Composition, $Y_O=0.08, Y_C = 0.01$
Feed Outlet	$u = U_{belt}$	Zero Gradient, $\delta T/\delta x=0$	Zero gradient, $\delta Y/\delta x=0$
Feed Top Surface	$u = U_{belt}$	Coupled Convective/Conduction and Radiation Heat Transfer	Specified Composition, $Y_{H_2}=0.2, Y_{N_2} = 0.8$
Feed Bottom Surface	$u = U_{belt}$	Contact Resistance $R = R_{spec} m^2K/W$	Zero gradient, $\delta Y/\delta y=0$
Belt Inlet	$u = U_{belt}$	Temperature Specified $T = 30^\circ C$	n.a.
Belt Outlet	$u = U_{belt}$	Zero Gradient, $\delta T/\delta x=0$	n.a.
Belt Bottom Surface	$u = U_{belt}$	Coupled Convective/Conduction and Radiation Heat Transfer	n.a.
Furnace External Surfaces	n.a.	Radiative/Convective Heat Transfer $U = 20 W/m^2K, T_{amb} = 30^\circ C$	n.a.
Heating Element Surfaces	$u = v = 0.0$	Temperature Specified ($T = 1050, 1150^\circ C$ for design)	n.a.

RESULTS – VALIDATION

Testwork at the existing QNPL reduction furnace and on a pilot scale facility at the CSIRO Clayton Laboratories provided data to validate the computational model.

Plant tray tests, using pre-prepared 30cm square trays of sawdust/calcine mix, yielded data of the final reduction extent and carbon content as a function of bed depth, sawdust mass fraction, belt speed, and furnace temperature profile. As the sample tray proceeded through the furnace, continuous measurements of the bed temperature at two depths were taken from thermocouples mounted within the sample tray.

Results showing the measured and computed temperature history for two runs with significantly different furnace temperature set-points are shown in Figures 3 and 4. Agreement between predictions and measurements is generally seen to be reasonable.

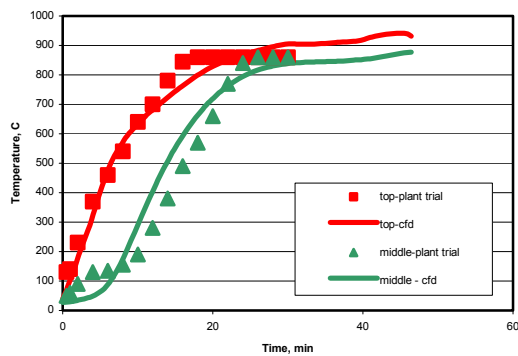


Figure 3: Temperature history at bed surface and at middle of bed depth. Thermocouple measurements from plant tray tests and corresponding computational model predictions

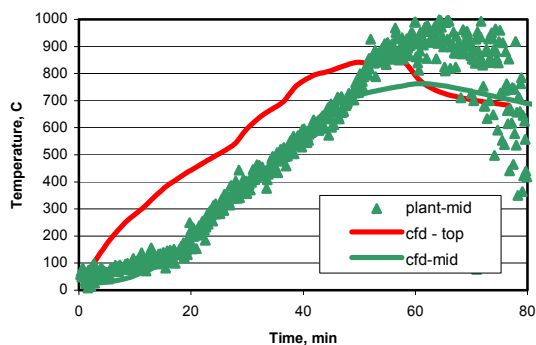


Figure 4: Computed temperature history at bed surface and at middle of bed depth. Thermocouple measurements from plant tray tests at middle of bed depth.

Figure 5 compares the measured and computed oxygen content of the reduced calcine for a series of five plant tests. Again model predictions are in reasonable agreement with the plant data. The final two data points shown in the figure are the observed and predicted calcine oxygen content for the pilot scale tests undertaken by the CSIRO at two different belt speeds. While the model

shows the correct trends the absolute levels are not well predicted for the CSIRO tests. One significant difference between the pilots scale and actual furnace is that the former has no provision for bottom heating of the charge material. It is this effect and the resulting uncertainty in the boundary condition prevailing at the bottom of the tray that is believed to be responsible for the poorer agreement in these cases.

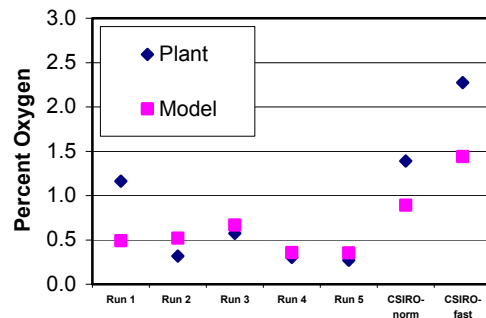


Figure 5: Measured and computed Oxygen content of furnace product.

RESULTS – PREDICTIONS

Up to this point the development and validation of the computational model is really only an academic exercise. The final (and from the client's perspective, most important) step is to use the model as a guide in optimising the process and to design the new furnace. In this regard Figure 6 illustrates the predicted temperature history and reduction profile for a new furnace designed to give the required production rate for bed depths of 30, 40, and 50 mm. Predictions of this type have been used to specify the operating bed depth and length of the new furnace. Other computations explored the effects of sawdust content, initial calcine composition, furnace temperature profiles and the sensitivity of the model to the specified kinetic parameters.

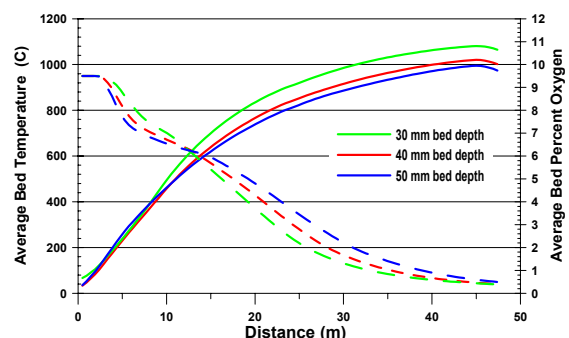


Figure 6: Predicted average bed temperature (solid lines) and oxygen content (dashed lines) for bed depths of 30, 40, and 50 mm.

Figure 7 shows the predicted cooling behaviour of the furnace charge which allows for an accurate determination of the furnace cooling zone length to ensure that material discharges from the furnace at a temperature suitable for safe handling by operators and downstream equipment.

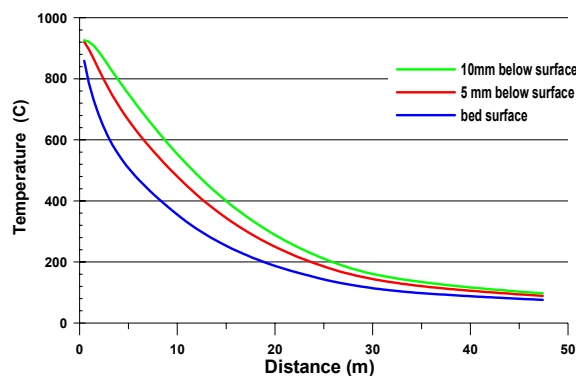


Figure 7: Predicted bed temperature distribution during cooling. Temperature predictions at the bed surface and at depths of 5 and 10 mm.

CONCLUSION

Through the use of UDS's a complex and industrially relevant thermochemical problem has been found to be tractable using a CFD model based on commercially available software. The model has been developed using experimentally determined thermo-physical properties and chemical kinetic parameters as required and validated against plant measurements and pilot scale experiments.

The model has yielded significant insight into the temperature and reduction profiles of nickel oxide powder under travelling-belt furnace process conditions. The model has provided benefit to process design by helping to clarify the effects of bed thickness and calcine composition and guidance in the design of the new furnace through specification of the required heating and cooling zone lengths and the required heating profile.

ACKNOWLEDGEMENTS

The author gratefully acknowledges the assistance of Grant Macgregor and Mark Fisher of QNPL Technical Services for performing the trials and analysis of the plant tray tests, David Harris and Dan Roberts at CSIRO Energy Technology for their assistance in determining the kinetic parameters for sawdust devolatilisation and gasification, and Robert Flann, CSIRO Minerals for performing the pilot scale reduction tests. Finally, the author would like to thank QNPL for assistance during the course of this work and kind permission for its publication.

REFERENCES

- HARRIS D.J. and SMITH I.W. (1990) "Intrinsic Reactivity of Petroleum Coke and Brown Coal Char to Carbon Dioxide, Steam and Oxygen". *Proc. Comb. Inst.* 23, 1185-1190
- HOOGSCHAGEN J. (1955) "Diffusion in Porous Catalysts and Absorbents." *Industrial and Eng. Chemistry.* Vol. 47, No.5, pp. 906-913.
- RASHED, A.H. and RAO Y.K. (1996) "Kinetics of Reduction of Nickel Oxide with Hydrogen in the 230-452 C Range". *Chem Eng Comm.*, 1996 Vol. 156, pp.1-30 2.
- ROBERTS D.G. and HARRIS D.J. (2000) "Char Gasification with O₂, CO₂ and H₂O: Effects of Pressure on Intrinsic Reaction Kinetics", *Energy & Fuels* 14(2), 483-489.